EAI Endorsed Transactions
on Pervasive Health and Technology
Research Article EAI.EU

A Soft Anthropomorphic & Tactile Fingertip for Low-Cost Prosthetic & Robotic Applications

E.L. Secco[1,*], C. Moutschen[2]

[1]Robotic Laboratory, Department of Mathematics & Computer Science, Liverpool Hope University, Hope Park L16 9JD, UK
[2]HELMo-Gramme University, Quai du Condroz, 28, 4031 Angleur, Belgium

Abstract

Nowadays, prosthetic and robotic hands have reached an amazing dexterity and grasping capability. However, to enhance a proper tactile 'experience', dexterity should be supported by proper sensation of daily life objects which such devices are supposed to manipulate. Here we propose a low cost anthropomorphic solution for the integration of a force sensor within a biologically inspired fingertip. A commercial force resistive sensor is embedded within a human-like soft fingertip made of silicone: the housing of the sensor - a 3D printed bay embedded within the fingertip - is analyzed via Finite Element Analysis and optimized to enhance sensor response. Experiments validate the design and proposed solution.

Keywords: Anthropomorphic Design, Biologically Inspired Design; Sensor Integration, Sensor Optimization.

Received on 28 June 2018, accepted on 04 July 2018, published on 23 July 2018

doi: 10.4108/eai.28-2-2018.155078

1. Introduction

In 2008, they were about 3 million of arm amputee people [1], due to congenital factors, tumours and diseases. In general, the principal reason of amputation involves traumatic events in more than 75% of all cases. According to the National Centre for Health Statistics [2], every year, in USA, there are about 50,000 new amputations. Therefore a significant number of patients are looking for proper artificial devices replacing their missing counter body parts and limbs.

Here we specifically focus on hand amputation and robotic or prosthetic hands which can support the recovery of a human hand dexterity and manipulation capability. According to current market and research on prosthetics, many devices have been already successfully developed [3]. Some of these devices exhibit very high manipulation capability [3-5], other ones show anthropomorphic design [6], high performant integration with force and tactile sensors [7] and further ones combine simplify design with relatively low-cost manufacturing [8].

Unfortunately, combining high performance with proper sensor integration and low cost is quite difficult. On average, most of these devices are quite expensive – in the order of tens of thousands of euro - they do not necessarily offer a set of embedded sensorial component; 'soft' interaction between the device itself and the manipulated objects may not be offered as well.

In this context, this paper presents the development of a low cost and affordable prosthetic hand which aims at offering an anthropomorphic design and experience to the amputee [9].

The paper is organized as it follows: the following section presents the main design of the hand and the integration of low cost tactile sensors combined with a soft fingertip artificial skin. A further section presents an experimental set-up where we optimize the design of the terminal parts of the fingers. Results are then discussed.

2. Design

The design of the hand is based on a 3D printing manufacturing process which is combined with the optimization of its fingers, since a low cost tactile sensor is integrated within the fingertip. This latter one is covered

*Corresponding author. Email:seccoe@hope.ac.uk

with a layer of silicone in order to enhance grasping capability and soft contact between the artificial finger and the manipulated object, as well as to increase the overall sensitivity of the sensor around the fingertip surface. A low-cost Force Resistive Sensor (FRS) is adopted. This one is covered by silicone, since this material is available at low cost and it can be easily moulded and adapted to fit the desired shapes. The overall approach of this design aims at performing a user-friendly experience of the device use in daily life.

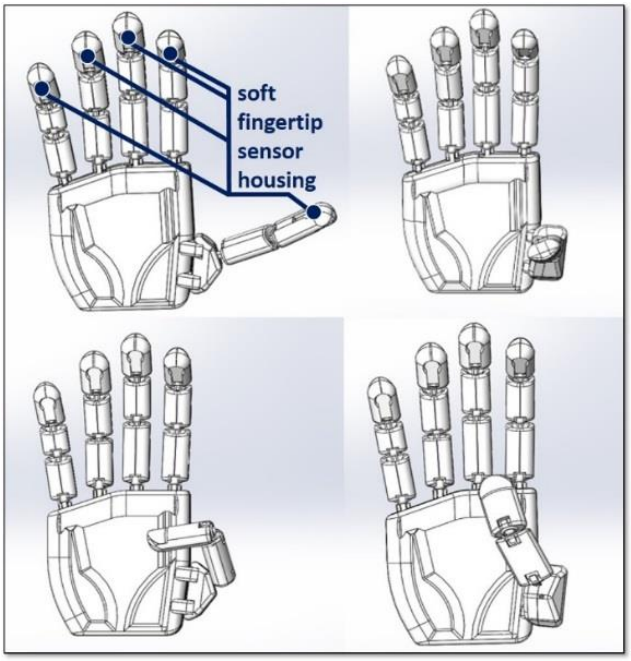

Figure 1. The anthropomorphic robotic and prosthetic hand.

2.1. Materials

The prosthetic hand, the palm, as well as the artificial finger were designed and printed in Acrylonitrile Butadiene Styrene (ABS) with a 3D printer (HP 3D Design jet). This material have good mechanical properties which allowed the simulation and performance of laboratory tests. An overall view of the design of the hand and of the finger of the hand is reported in the Figures 1 and 2.

Figure 2 shows an overview of the finger and of the housing for the tactile sensor. It can be noticed that the ABS material is quite solid and rigid to house a tactile sensor and then test the sensor: the transducer, in fact, will have a rigid support which will not be deformed in case of the application of load. This is important in view of testing the sensor and obtaining reliable measurements.

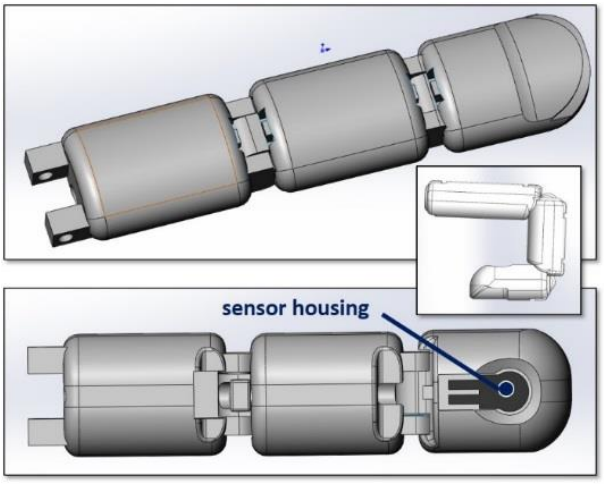

Figure 2. The anthropomorphic robotic finger and fingertip sensor housing.

On the contrary, in view of applying a silicon layer on top of the sensor, it is important to notice that the softness of this material will introduce some concerns about the repeatability of the measurements when loads will be applied.

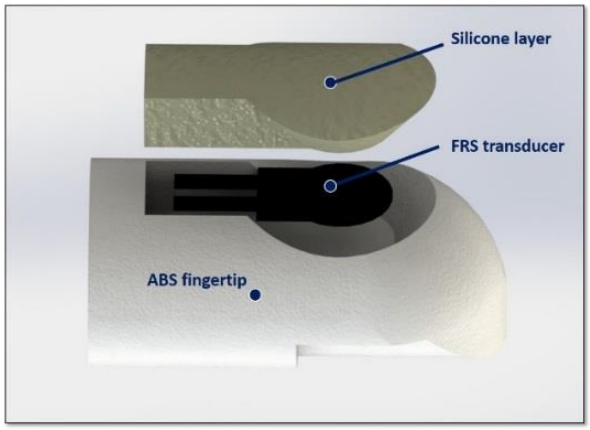

Figure 3. The sandwich layers configuration around the tactile sensor.

The displacement of the silicon layer was made of an EcoFlex 50 platinum-catalysed silicon [10]: the silicone was prepared by mixing two parts which were stirred and moulded on the sensor housing of the 3D printed fingertip. Figure 3 shows the overall design of the fingertip, combining the BAS support, the FRS component and finally the artificial skin layer of silicone.

2.2. Selection of the manufacturing material and technology

In order to optimize the design of the FRS support, it is important to have an under layer which is robust and rigid: as it was mentioned before, the ABS material has good mechanical properties and – at the same time - it allows the flexibility of changing the design of the support via the 3D printing process. Moreover, the ABS material has a reasonable density which makes possible to have a quite light prosthetic device (Table 1).

Thanks to this approach, we will be able to quickly design, manufacture, test and re-design different forms: such a strategy would not be easily obtainable by using others manufacturing technologies (e.g. modelling, sculpting). Moreover, this approach has also the befit of keeping the cost of the process quite restrained.

	Property	*Value*	*Units*
ABS (Acrylonitrile Butadiene Styrene)	Elastic Modulus	$234 \cdot 10^6$	*N/m*
	Poisson's Ratio	0.35	-
	Mass Density	1040	Kg/m^3

Table 1. The ABS mechanical properties.

2.3. Design and selection of the sensor

The proposed sensor is a Model 400 Force Resistive Sensor (FSR), short version, from Interlink Electronics [11]. This device is characterized by a small size which is combined with good properties to be embedded within the hand fingertip. Moreover it has proper electrical characteristics and weight for this application.

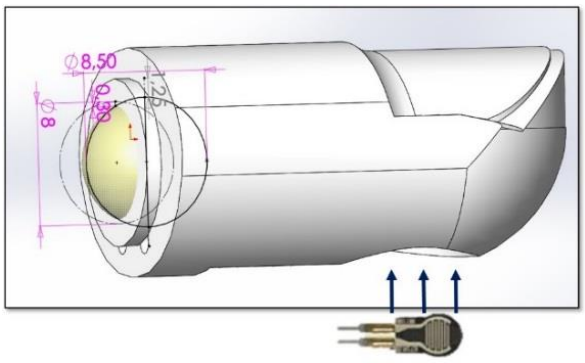

Figure 4. The FSR 400 Short sensor embedded within the fingertip.

The sensor has a force range of 0.2 – 20 N based. Sensor output change is produced by pressing the device which has the effect of changing and increasing the resistance of the sensor layer and therefore its electrical response. This electrical change can be correlated to the pressure in order to infer the effective process, provided that the sensor has been calibrated.

According to the sensor specifications, the electrical current has to be limited within a value of less than 1 mA per square centimetre applied force. Even if the inter-sensor repeatability is quite low (6%), nevertheless a significant hysteresis of more than 10% may be observed. In this context, it is important to notice that the resistance of the sensor may be affected by changes in the order of 10% during time. Despite these limitations, this device has proper characteristics for the proposed implementation: it can be positioned on the sensor housing of the artificial finger and be used in daily life scenario where the end-user is manipulating objects and performing typical daily actions like grasping a glass or handling a tool.

2.4. Human-like skin

Our human limbs and hands are made of soft tissues and skin. Such a softness is strongly involved on the interactions with objects since it allows the tissue to be deformed and adapt while in contact with external items. Because of that, we explored the possibility to recover the proposed design with a layer of soft silicone, which should enhance the bio-mimetic of the device itself. There are multiple advantages on adopting such a solution:

- End-user will benefit from a more realistic sensation.
- Silicone will intrinsically distribute the external force before transferring this stimulus to the underneath sensor
- A soft touch could be used in relation to the daily usage of touch screen by the user (i.e. mobile phone, tablet, etc.)

According to these benefits, a two components platinum-catalyzed silicones, EcoFlex 50 - SmoothOn, [10] - was used. In order to predict the mechanical response of this material vs contact force on the fingertip, a set of mechanical properties have to be defined, according to the following parameters:

Elastic module	=	2172000 N/m
Poisson's ratio	=	0.49
Density	=	716.9 kg/m1

3. Optimization – FEA Simulations & Laboratory Trials

The sensor housing was designed by considering different shapes in order to optimize the response of the sensor within the housing. The housing shape, in fact, can condition the way in which the external applied force (i.e. the contact force between the object and the fingertip) is

transferred to the sensor through the silicone layer in between.
In order to optimize the housing design, laboratory trials with different shapes were performed: 4 configurations and shapes of the housing were tested. For each configuration, a 3D printed model of the fingertip was designed, printed and integrated with the silicon layer before the tests. The 4 configurations' design were tailored in function of two design parameters, namely the external radius of the housing bay and the depth of the bay. Figure 5 shows the geometry of the housing and the two aforementioned parameters.

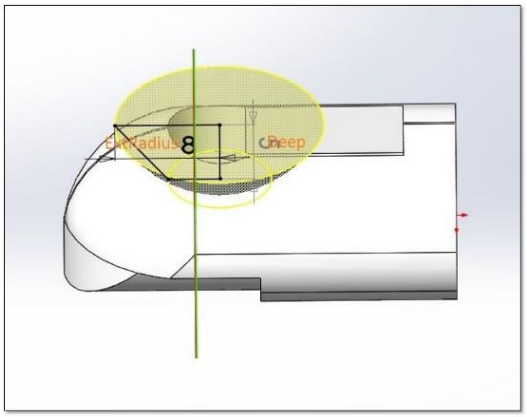

Figure 5. The fingertip silicon bay and the two geometrical parameters, namely the radius and depth of the sensor housing.

A two stages process was followed for the optimization of the geometry: first of all the effect of the shape was tested via a Finite Element Analysis (FEA) which was predicting the force distribution on the tip of the finger vs. applied simulated load. Secondly, a real set of experiments were performed were the fingertip and sensor housing was loaded with a set of weight and the sensor output was measured returning an estimation of the effective applied force thanks to a calibration curve of the sensor. Results of all these simulated and real testes were then finally compare din order to select the most appropriate and optimized configuration of the sensor housing and fingertip design.

3.1. Experimental Set-up

3.1.1. Measurements

In order to perform experimental measurements, an additional resistor of 10 kOhm (RM) was integrated in the circuit: the resistance of the sensor (FRS) changes according to the applied load and it decreases the more the load is applied. Assuming a constant power supply of 5 Volts (V_+), therefore the current (I_1) increases as soon as the resistance decreases, establishing a linear correlation between the force and the resistance. Therefore, it holds:

$$\begin{aligned} V+ &= I1(RM+FSR) \\ \iff I1 &= \frac{V+}{RM+FSR} \end{aligned} \quad (1)$$

$$\begin{aligned} VOut &= I2 * RM \\ \iff I2 &= \frac{VOut}{RM} \end{aligned} \quad (2)$$

Where I_2 and V_{out} are the output current and voltage, respectively. Since I_1 is equal to I_2, then it also holds:

$$\begin{aligned} \frac{V+}{RM+FSR} &= \frac{VOut}{RM} \\ \iff FSR &= \frac{V+ * RM}{VOut} - RM \end{aligned} \quad (3)$$

Finally, since RM and V_+ are equal to 10 kOhms and 5 V, respectively, then V_{out} can be easily acquired via a Data Acquisition (DAQ) system. For the purpose of this project, a low-cost and easily customizable DAQ system was used, namely an open-source Arduino platform.

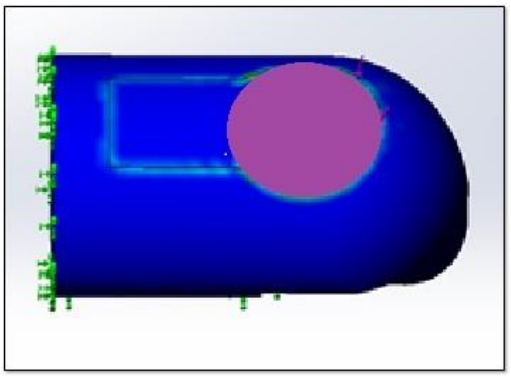

Figure 6. The fingertip tactile sensitive area.

3.1.2. Selection of the additional resistor

The RM value affects the sensor calibration curve: the lower is the RM resistance, the higher is the precision of the sensor reading when we apply high load. On the contrary, higher precision vs. low load can be obtained by reducing the RM resistance value. According to the type of application that we are considering, a good compromise is to choose a resistance of 10 kOhms, which allows good performance vs. loads in the order of 200 gr (i.e. the weight

of a typical manipulated daily life object). Clearly a different application may require the use of a different additional resistor, which can be easily changed within the proposed circuit.

3.2. Finite Element Analysis (FEA)

A Finite Element Analysis (FEA) allows predicting the sensor behavior vs. the applied loads and the different configurations and shapes of the sensor housing. Particularly, the FEA should predict the effective load which is applied to the transducer under the soft layer.

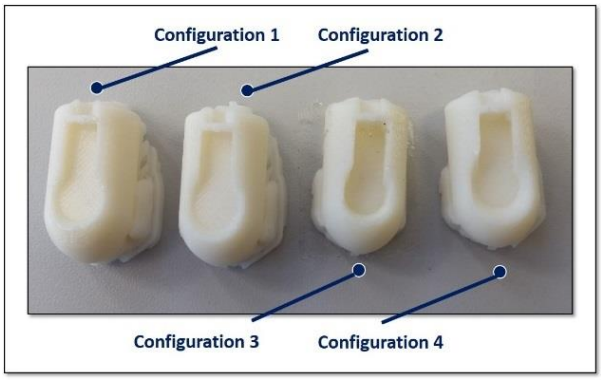

Figure 7. The four different configurations of the tactile bay: from the left to the right, the Deep3R6, Deep3R8, Deep5R6 and Deep5R8 configurations, respectively (details in par. 3.2).

The FEA is performed with SolidWorks software (Dassault Systèmes SOLIDWORKS Corp.) by defining the fingertip design as it is reported in Figure 6: the left green arrows within the figure refers to the constraints, whereas the surface of contact between the silicone layer and the sensor housing is defined as a global contact without penetration. A 20 N load is simulated and applied to the fingertip: such a load is assumed to be uniformly distributed over the silicone layer, precisely the circular surface, which is reported in purple color in the figure. A circular tactile sensitive was adopted in order to mimic the underlayer shape of the FRS circular sensor.

Four configurations of the sensor housing were designed and prototyped, according to different external radius of the housing – namely a 6 mm and 8 mm radius, respectively – and two values of the depth of the housing – i.e. 3 mm and 5 mm, respectively (Figure 7).

3.2.1. FEA of the Deep3R6 sensor housing

This first FEA simulation experiment was performed with a sensor housing having an inner depth of 3 mm and an external top radius of 6 mm: this configuration was labelled as *Deep3R6*, where the first part of the label – i.e. *Deep3* - refers to the depth of the housing and the second part of the label (*R6*) refers to the radius (*R*). The same strategy was used to label the other sensor housing configuration.

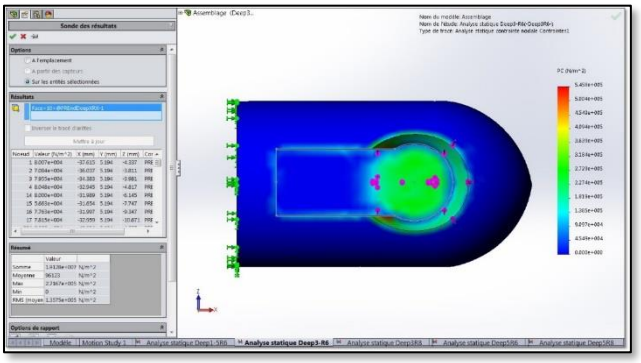

Figure 8. FEA simulation of the pressure distribution on the *Deep3R6* sensor housing.

Figure 8 report the results of the FEA simulation, assuming an overall uniformly distributed load of 20 N over all the fingertip surface (i.e. the sensor area and the crown area). The sensor is covered by a layer of silicone, whose mechanical properties of the FEA simulation have been reported in Table 1. Accordingly, the figure shows the pressure distribution on the sensor housing. The following results were performed via the FEA:

- Area of the sensor
  = 121.54 mm
- Crown area (delimited by external walls)
  = 48 mm
- Average specific pressure on sensor
  = $0.96 \cdot 10^5$ N/mm
- Average specific pressure on crown
  = $1.74 \cdot 10^5$ N/mm

Accordingly, it holds:

- Sensor force
  = 121,54·0,96·0,1 = 11,68 N
- Dissipated force
  = 48,48·1,74·0,1 = 8,44 N
- Percentage of the measured force
  = 11,68/(8,44+11,68)·100 = 58,05 %

Where the percentage of the measured force measures the effective percentage of the load, which is pushing on the sensitive area of the sensor. A summary of these results is also reported on Table 2.

Part	*Area*	*Average Pressure*	*Force*	*Measured Force*
	[mm²]	*[N/mm²]*	*[N]*	*%*
Sensor Area	121.54	$0.96 \cdot 10^5$	11.68	58.05
Crown Area	48	$1.74 \cdot 10^5$	8.44	-

Table 2. Percentage of forces which is applied to the sensor when using the *Deep3R6* sensor housing.

According to these results, more than 40% of the applied force is lost, namely the precision of the measurement at the sensor level may have to be multiplied by a factor of 1.4. It is important to notice that these results are affected by intrinsic errors of due to the FEA numerical process: in particular, it should be notice that the overall sum of the force repartition (11.68 N on the senor area and 8.44 N on the crown area) is not equal to 20.0 N (namely it is 20.12 N).

A similar FEA simulation was performed with the other fingertip configuration of the sensor housing in order to establish the repartition of the force.

3.2.2. FEA of the Deep3R8 sensor housing

The FEA simulation was performed assuming a top radius of 8 mm and inner depth of 3 mm of the sensor housing. The same hypothesis were adopted in terms of the mechanical properties of the silicone and the uniformly distribution of the load. Table 3 reports the results of this latter simulation, suggesting that a larger housing (i.e. an 8 mm radius vs a 6 mm radius) may provide a larger dispersion of the force, namely a lower percentage of the effective measured force (55.04% vs. 58.05%). In this latter case, in fact, the simulation predicts a loss of 45% of the applied force, namely an uncertainty factor of the measurements of 1.45.

Part	*Area*	*Average Pressure*	*Force*	*Measured Force*
	[mm²]	*[N/mm²]*	*[N]*	*%*
Sensor Area	121.54	$0.97 \cdot 10^5$	10.54	55.04
Crown Area	61.11	$1.41 \cdot 10^5$	8.61	-

Table 3. Percentage of forces which is applied to the sensor when using the *Deep3R8* sensor housing.

3.2.3. FEA of the Deep5R6 sensor housing

A further simulation was performed with a deep of 5 mm and a top radius of 6 mm, showing that a 5 mm layer of silicon significantly affect the performance of the sensor when compared to the previous configuration assuming a layer of only 3 mm thickness (42.57% vs. 55.04% and 58.05%, respectively).

Part	*Area*	*Average Pressure*	*Force*	*Measured Force*
	[mm²]	*[N/mm²]*	*[N]*	*%*
Sensor Area	121.54	$0.99 \cdot 10^5$	12.09	42.57
Crown Area	89.34	$1.83 \cdot 10^5$	16.31	-

Table 4. Percentage of forces which is applied to the sensor when using the *Deep5R6* sensor housing.

3.2.4. FEA of the Deep5R8 sensor housing

Finally, the last simulation was performed with a deep of 5 mm and a top radius of 8 mm. Here, the FEA predicts the worst scenario where the reduction of the measured force in terms of percentage is more than 60% of the applied force.

Part	*Area*	*Average Pressure*	*Force*	*Measured Force*
	[mm²]	*[N/mm²]*	*[N]*	*%*
Sensor Area	121.54	$0.71 \cdot 10^5$	8.57	39.42
Crown Area	104.77	$1.26 \cdot 10^5$	13.17	-

Table 5. Percentage of forces which is applied to the sensor when using the *Deep5R8* sensor housing.

3.2.5. FEA simulations: results & design optimization

According to the FEA simulations, we may predict that increasing the value of the depth and radius of the sensor housing will significantly weaken the perceived force at sensor level, and therefore affect the precision of the measurement. On the other side, the benefit of a larger value of the radius is on having a larger sensitive surface where the applied load can be applied, which inherently makes the fingertip (and the sensor) capable to face higher load without being damaged or saturated: attenuating the load by a factor of 2 would allow us measuring two times heaviest forces.

On the contrary, in terms of precision, the optimal design should be the one with the smallest depth and radius, namely the *Deep3R6* configuration.

A set of real experiments may support us on taking a proper decision and find the best optimal compromise.

3.3. Physical experiments - validation

In order to validate the FEA simulations, physical experiments were performed. These trials also allow to

double check if the results from the FEA simulations were reliable vs. different positioning of the applied load on the fingertip. The simulations, in fact, were performed under the simplified hypothesis that the load was uniformly distributed over the fingertip surface. To perform the test, a customized equipment was designed and 4D printed. Tests were also performed without the silicon layer in order to evaluate the effective contribution of this layer on the response of the sensor.

Figure 9 shows the 3D design of the equipment which allows loading the fingertip with desired force: the applied force is obtained by using a set of metal weights. This set-up was designed to provide a system for the execution of repeated measurements. After designing the system, it was printed in ABS material (see top panel of the Figure). The mass of this set-up was equal to 33.02 gr. Each measurement, namely each applied weight, was performed 3 times. The sensor signal – i.e. the output in voltage - was acquired via the Arduino board and the average of the three measurements were reported.

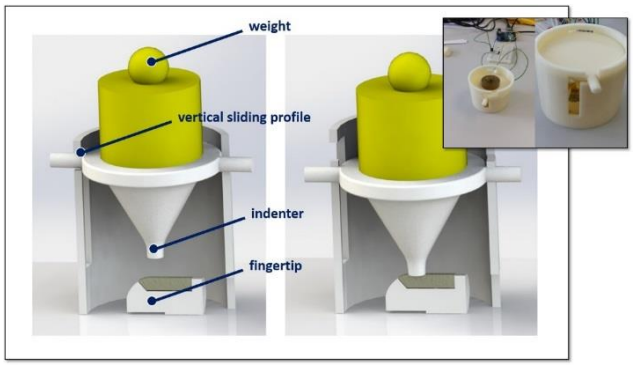

Figure 9. Design of the experimental equipment of testing the fingertip sensor with real load. On the top right panel of the figure is reported the manufactured equipment.

3.3.1. Tests without the silicone skin

The first set of trials was performed without depositing the silicon layer over the sensor. The purpose of this set of trials was to validate the sensor without introducing any interference between the transducer and the applied loads. Loads were applied from a value of 50 gr to a final value of 3 kg, considering the intrinsic weight of the equipment as well. Table 6 reports the masses of the applied weight and the sensor response.

According to these results, it was noticed that the repeatability of the measurements was not very high during some of the trials, due to slightly different positioning of the load on top of the experimental set-up, i.e. the plate supporting the weights in Figure 9.

In this context, adding a layer of silicone on top of the sensor, should help on stabilizing the measurement and output of the sensor vs. little change on the position of the weight vs the barycentre of the sensor.

The silicon, in fact, is intrinsically viscoelastic and should compensate with a damping effect. Moreover, this soft layer should distribute the force and provide a more human-like response on the sensor.

Mass	***Voltage***	***RFSR***
[gr]	***[V]***	***[Ohm]***
53.02	0.35	132857
	0.33	141515
	0.34	137059
Average	*0.34*	*137144*
83.02	0.55	80909
	0.56	79286
	0.56	79286
Average	*0.56*	*79827*
133.02	0.72	59444
	0.72	59444
	0.72	59444
Average	*0.72*	*59444*
233.02	1.16	33103
	1.06	37170
	1.07	36729
Average	*1.10*	*35667*
533.02	1.37	*26496*
	1.37	*26496*
	1.39	*25971*
Average	*1.38*	*26321*
1033.02	2.51	*9920*
	2.63	*9011*
	2.64	*8939*
Average	*2.59*	*9290*
2033.02	3.05	*6393*
	2.96	*6892*
	2.93	*7065*
Average	*2.98*	*6783*
3033.02	3.41	*4663*
	3.40	*4706*
	3.35	*4925*
Average	*3.39*	*4765*

Table 6. Response of the sensor vs. the applied loads on fingertip without the silicone layer.

3.3.2. Tests with embedded silicone skin, *Deep3R6* and *Deep3R8* configurations

Finally, the fingertip was prepared and covered by a silicone layer, and trials were performed as well. Figure 10 shows the final appearance of the fingertip when equipped with the artificial skin.

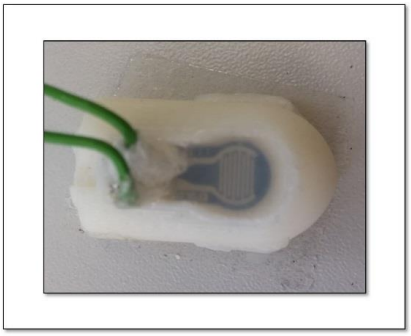

Figure 10. Example of the fingertip embedding the immersed sensor with the silicone layer on top.

Table 7, left panel reports the experimental results: it can be notice that the repeatability of the measurement has significantly improved when compared to the same load applied to the sensor without any silicone. Similar results were obtained with the Deep3R8 configuration (right panel of Table 7).

Mass	*Voltage*	*RFSR*
[gr]	*[V]*	*[Ohm]*
53.02	0.34	137059
	0.35	132857
	0.35	132857
Average	*0.35*	*134258*
83.02	0.90	45556
	0.90	45556
	0.91	44945
Average	*0.90*	*45352*
133.02	1.71	19240
	1.67	19940
	1.69	19586
Average	*1.69*	*19589*
233.02	2.45	10408
	2.45	10408
	2.44	10492
Average	*2.45*	*10436*
533.02	3.39	4749
	3.40	4706
	3.40	4706
Average	*3.40*	*4720*
1033.02	3.91	2788
	3.90	2821
	3.90	2821
Average	*3.90*	*2810*
2033.02	4.20	1905
	4.20	1905
	4.19	1933
Average	*4.20*	*1914*
3033.02	4.25	1765
	4.29	1655
	4.31	1601
Average	*4.28*	*1674*

Mass	*Voltage*	*RFSR*
[gr]	*[V]*	*[Ohm]*
53.02	0.00	NA
	0.00	NA
	0.00	NA
Average	*0.00*	*NA*
83.02	0.00	NA
	0.00	NA
	0.00	NA
Average	*0.00*	*NA*
133.02	0.00	NA
	0.00	NA
	0.00	NA
Average	*0.00*	*NA*
233.02	0.26	182308
	0.19	253158
	0.03	1656667
Average	*0.16*	*697377*
533.02	2.37	11097
	2.39	10921
	2.38	11008
Average	*2.38*	*11009*
1033.02	3.11	6077
	3.14	5924
	3.15	5873
Average	*3.13*	*5958*
2033.02	4.13	2107
	4.15	2048
	4.15	2048
Average	*4.14*	*2068*
3033.02	4.16	2019
	4.18	1962
	4.18	1962
Average	*4.17*	*1981*

Table 7. Response of the sensor vs. the applied loads on *Deep3R6* and *Deep3R8* sensor housing with silicone layer (left and right panels, respectively).

3.3.3. Tests with embedded silicone skin, *Deep5R6* and *Deep5R8* configurations

Table 8, left and right panels, refers to the homologues results when adopting the Deep5R6 and Deep5R8 configurations, respectively.

Mass	*Voltage*	*RFSR*
[gr]	*[V]*	*[Ohm]*
53.02	0.00	NA
	0.00	NA
	0.00	NA
Average	*0.00*	*NA*
83.02	0.00	NA
	0.00	NA
	0.00	NA
Average	*0.00*	*NA*
133.02	0.00	NA
	0.00	NA
	0.00	NA
Average	*0.00*	*NA*
233.02	0.00	NA
	0.00	NA
	0.00	NA
Average	*0.00*	*NA*
533.02	1.84	17174
	1.78	18090
	1.84	17174
Average	*1.82*	*17479*
1033.02	3.10	6129
	3.09	6181
	3.10	6129
Average	*3.10*	*6146*
2033.02	3.77	3263
	3.76	3298
	3.75	3333
Average	*3.76*	*3298*
3033.02	4.15	2048
	4.15	2048
	4.16	2019
Average	*4.15*	*2039*

Mass	*Voltage*	*RFSR*
[gr]	*[V]*	*[Ohm]*
53.02	0.00	NA
	0.00	NA
	0.00	NA
Average	*0.00*	*NA*
83.02	0.00	NA
	0.00	NA
	0.00	NA
Average	*0.00*	*NA*
133.02	0.00	NA
	0.00	NA
	0.00	NA
Average	*0.00*	*NA*
233.02	0.00	NA
	0.00	NA
	0.00	NA
Average	*0.00*	*NA*
533.02	1.58	21646
	1.62	20864
	1.61	21056
Average	*1.60*	*21189*
1033.02	2.76	8116
	2.77	8051
	2.77	8051
Average	*2.77*	*8072*
2033.02	3.71	3477
	3.70	3514
	3.64	3736
Average	*3.68*	*3576*
3033.02	4.15	2048
	4.15	2048
	4.16	2019
Average	*4.15*	*2039*

Table 8. Response of the sensor vs. the applied loads on *Deep5R6* and *Deep5R8* sensor housing with silicone layer (left and right panels, respectively).

3.3.4. Results summary

According to all trials which were performed without the silicon and with the silicone bay in the 4 different configurations, an overall summary of the results was plotted, as it is reported in Figure 11.

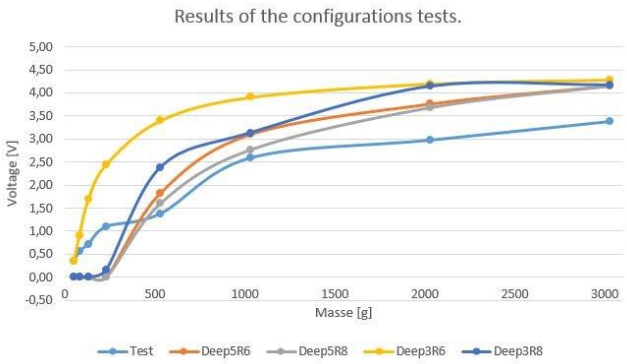

Figure 11. Overall behaviour of the sensor response vs the different experimental configurations. The blue Test plot refers to the test as performed without any silicon layer).

According to this summary plot, it can be observed that the 'without silicone' configuration – i.e. the blue curve – is not very acceptable, due to its unregular pattern. On the contrary, the yellow curve (i.e. the *Deep3R6*) shows a very regular pattern which is quite desirable as a sensor response. The repeatability of the measurements which were performed with the Deep3R8 configuration was quite low: this is well reflected on the curve within the graph of the figure as well. Similar observations can be reported vs the other curves, apart from the aforementioned response of the *Deep3R6* set up, which is proved to be the best response in terms of regularity of the curve. Nevertheless, this configuration has a good performance and sensitivity at low weight, but it shows a very low sensitivity as soon as the load is incremented and it approaches values in the order of 500 gr. This latter drawback may be solved by compensating the reduction of the sensitivity with a chance of the additional resistor (see also par. 3.1.2).

4. Discussion & conclusion

From a comparison between the results of the FEA simulations and the results of the experimental trials, it can be noticed that the higher are the curves of Figure 11, the lower is the error between the predictions of the simulations and the effective real response of the sensor. In other words, the lower is the dissipation of the force, the higher is the reliability of the prediction.

Taking on board these results, together with the outcome of the FEA simulations and of the real experiments, we can select as optimal solution the configuration Deep3R6, namely a sensor bay of silicone with a depth of 3 mm and an external radius of 6 mm. Qualitatively, this is also the configuration which provides a 'human-like' fingertip sensation when the artificial fingertip is pressed by a human subject. An higher depth, in fact, provides a 'too soft' sensation on the tip which causes an higher dissipation of the force.

Finally, we proposed a human-like silicone based fingertip for artificial hand: the fingertip embeds a low cost sensor – in the order of 5 USD – which allows a proper calibration in the typical range of force of manipulated daily life objects. The proposed solution maybe synergic integrated with a proper grasping control of the hand [12-16]. It also offers the possibility of a better grasping capability which is combined with the benefit of having a human-like soft sensation of the finger when getting in contact with another human hand. A selection of different values of the additional resistor will allow the end-user to tailor the senor response within other range of force, according to the type of applications and tasks to be performed by the hand.

Acknowledgements

This work was presented in thesis form in fulfilment of the requirements for the MSC in Computer Science for the student Cedric Moutschen under the supervision of E.L. Secco from the Robotics Laboratory, Department of Mathematics & Computer Science, Liverpool Hope University and of S. Frederick from the Industrial Engineering Department, Helmo Gramme (BE).

References

[1] LeBlanc M., MSME, CP, "Give Hope – Give a Hand" (2008), Available at: https://web.stanford.edu/class/engr110/2011/LeBlanc −03a.pdf (Accessed: 1 May 2016)

[2] "Statistics on hand and arm loss", In: ISHN Magazine (2014), Available at: https://web.stanford.edu/class/engr110/2011/LeBlanc−03a.pdf (Accessed: 1 May 2016).

[3] Prensilia (2018) Available at: https://www.prensilia.com/ (Accessed: 14 March 2018)

[4] TouchBionics (2017) Available at: http://www.touchbionics.com/ (Accessed: 13 January 2017)

[5] GmbH S. "SCHUNK mobile Greifsysteme" (2018). Available at: http://www.schunk-modular-robotics.com/fileadmin/user_upload/PDF_Downloads/Mobile_Greifsysteme_2014_DE_WEB-PDF.pdf (Accessed: 5 April 2018).

[6] Secco E.L., Magenes G., "Bio-mimetic Finger - Human like morphology, control & motion planning for intelligent robot & prosthesis in Mobile Robotics", In: Moving Intelligence (2006) pp. 325–348, http://www.ars−journal.com/Mobile Robotics.html

[7] The Shadow Robot Company (2017) Available at: https://www.shadowrobot.com/products/dexterous-hand/ (Accessed: 17 October 2017)

[8] Open Bionics (2018) Available at: https://openbionics.com/ (Accessed: 6 February 2018)

[9] Moutschen C. (2016) Development of a sustainable and biologically inspired prosthetic hand. Master Thesis Dissertation, Liverpool Hope University & Helmo Gramme

[10] Smooth-On (2018) Available at: https://www.smooth-on.com/tb/files/ECOFLEX_SERIES_TB.pdf (Accessed: 5 April 2018)

[11] Interlink Electronics (2018) Available at: https://www.interlinkelectronics.com/fsr-400-short (Accessed: 6 April 2018)

[12] Magenes G, Passaglia F, Secco EL (2008) A new approach of multi-d.o.f. prosthetic control, 30th Annual Int Conf of the IEEE Eng in Medicine and Biology Society (EMBC), 3443-3446

[13] Matrone G, Cipriani C, Secco EL, Carrozza MC, Magenes G (2009) Bio-Inspired Controller for a Dexterous Prosthetic Hand Based on Principal Component Analysis, 31st Annual Int Conf of the IEEE Eng in Medicine and Biology Society (EMBC), 5022-5025

[14] Matrone G, Cipriani C, Secco EL, Magenes G, Carrozza MC (2010) Principal Components Analysis based control of a multi-DoF underactuated prosthetic hand, J of NeuroEng & Rehab, 7:16

[15] Matrone G, Cipriani C, Secco EL, Carrozza MC, Magenes G (2009) A biomimetic approach based on principal components analysis for multi-dof prosthetic hand control, Workshop CORNER, Genova, IT

[16] Matrone G, Cipriani C, Secco EL, Carrozza MC, Magenes G (2010) A dimensionality reduction strategy for dexterous prosthetic hand control, GNB, Torino, IT